Identification of Radius-Vector Functions of Interface Evolution for Star-Shaped Crystal Growth

Y. Zhao, D.Coca, S.A. Billings, Y.Guo, R.I.Ristic, L.L.De Matos, A.Dougherty

Research Report No. 1022

Department of Automatic Control and Systems Engineering
The University of Sheffield
Mappin Street, Sheffield,
S1 3JD, UK

October, 2010

Identification of Radius-Vector Functions of Interface Evolution for Star-Shaped Crystal Growth

Y.Zhao, D.Coca, S.A.Billings, Y.Guo *, R.I.Ristic, L.L.DeMatos †, A.Dougherty ‡

October 26, 2010

Abstract

This paper introduces a new method based on a radius-vector function for identifying the spatio-temporal transition rule of star-shaped crystal growth directly from experimental crystal growth imaging data. From the morphology point of view, the growth is decomposed as initial conditions, uniform growth and directional growth, which is represented by a static polynomial model based on the Fourier expansion. A recursive model is also introduced to help understand the dynamic characteristics of the observed systems. The applicability of the proposed approach is demonstrated using data from a simulation and from a real crystal growth experiment.

1 Introduction

Considerable theoretical and experimental effort has been expended in an attempt to develop a better understanding of growth processes that are driven by surface energy at the curved phase boundary. One of the most common examples of such a process is the growth of crystals. The crystal growth process starts at the nucleation stage, when several atoms or molecules form clusters that subsequently grow by the addition of other atoms. Patterns generated by growth processes are typically characterized in terms of characteristic length, (such as the thickness of a branch, the distance between two side-branches and the curvature of the branch tips) and crystal growth rate. The investigation of the time evolution of the characteristic lengths, using experimental, theoretical and computer simulation methods can provide valuable information on the mechanisms of crystal growth [R.Kobayashi, 1993; Dougherty and Lahir, 2005; Bisker-Leib and Doherty, 2001, 2003].

*Department of Automatic Control and System Engineering, University of Sheffield, UK.

†Department of Chemical and Process Engineering, University of Sheffield, UK.

‡Department of Physics, Lafayette College, USA.

A wide range of mathematical models have already been developed to simulate the growth dynamics of crystals. The Eden model [Eden, 1956a,b], initially developed to investigate the growth of biological cell colonies, and the diffusion-limited aggregation (DLA) model [Witten and Sander, 1981], one of the most striking examples of the generation of a complex disorderly pattern by a simple model, have been widely used in biology, colloid science and materials science [T.Williams and R.Rjerknes, 1972; D.Mollison, 1972; P.Meakin, 1983; M.J.Vold, 1963]. Recently, the Phase Field Model [R.Kobayashi, 1993] has been widely used in the simulation of the growth of alloys [George and Warren, 2002; Takaki et al., 2005; Hou et al., 2005]. Moreover, the Sharp Interface Model [Maalmi et al., 1995; M and M, 2007], the Boolean Model for Snowflake Growth [S.A.Wolfram, 2002] and the Cellular Automata Model [Zhao et al., 2009] have also been developed to model growth processes. A parabolic model with fourth-order correction was introduced to fit to the profile of the tips of NH4Cl dendrites [Dougherty and Lahir, 2005; A and T, 2007]. However, very few authors have studied the problem of how to obtain simple empirical mathematical descriptions directly from observed experimental growth data. The identification of the models of crystal growth directly from experimental observation is a powerful tool for understanding crystal growth mechanisms and for unravelling the complex relationships between various growth patterns and the environmental variables that control this process allowing for the development of robust model-based feedback control schemes.

Initially, this paper introduces a general model based on the polar coordinates which is parameterised by the arc length of contour. Theoretically, this model can describe an arbitrary closed contour. This paper then proposes a new approach to identify a radius-vector based function, as a particular case of the general model, directly from experimental observations (imaging) for star-shaped growth, which typical arises in the early stages of crystal growth. The *star-shape* is defined as: for any point in the contour p the whole line segment from the reference point O to p lies within the pattern. The reference point O is located in the interior of the contour. It is a criterion to test if a particular data set can be modelled by the proposed radius-vector based model. The distance from the pole of the polar coordinates is modelled by introducing a Fourier expansion, and the evolution characteristics are represented by a recursive model obtained by choosing the significant terms using the Error Reduction Ratio from the Orthogonal Least Square method [M.Korenberg and S.A.Billings, 1988].

The study begins in Sec.2 with the parameterisation of the contour of a crystal, and a description of the radius-vector function following a Fourier expansion. Section 3 introduces the model identification routine which is applied to a simulation example, followed by an application to the identification of a real example of NH_4Cl growth. Finally, conclusions are give in Sec.4.

2 Radius-Vector Function

Most currently studied methods in modelling crystal growth are based on cartesian coordinates. From the morphology point of view, this paper introduces a radius-vector based model in polar coordinates to identify the crystal growth processes in a polynomial form in terms of the characteristics of the growth speed of the interface.

In two dimensions, at a time t, the crystal is assumed to occupy an open subset $\Omega_t \in \mathbb{R}^2$ with contour represented by an evolving closed curve $\gamma(t)$ separating its interior and exterior. Now consider the closed contour curve in polar coordinates, which can be mapped as $\bar{x} : [0, S) \times (0, T) \rightarrow \mathbb{R}^2$ such that $\bar{x}(s,t) = \big(r(s,t), \theta(s,t)\big)$ is a point on the curve $\gamma(t)$ and $\bar{x}(0,t) = \bar{x}(S,t)$, $0 \leq \ s \leq S$, where r denotes the distance to the pole, θ denotes the positive angle required to reach the point from 0° and S denotes the arc length of $\gamma(t)$. The curve is parameterised so that the interior is on the left in the direction of increasing s (counter clockwise parameterisation). If $\big(r(s,t), \theta(s,t)\big)$ are given, then evolution of the contour can be completely reconstructed.

In this paper, to simplify the problem, $\theta(s,t)$ is assumed to be independent to t and is expressed as:

$$\theta(s,t) = \theta(s) = \frac{s}{S} \times 2\pi \tag{1}$$

As S is a constant, s is linear in θ. Therefore, $r(s,t)$ is a function between the radius r and the vector θ which determines the spatio-temporal evolution of the interface. In other word, the map $\gamma(t) \rightarrow \big(r(s,t), \theta(s,t)\big)$ can be simplified as the map $\gamma(t) \rightarrow r(s,t)$.

From the morphology point of view, this paper introduces a polynomial model expressed as

$$r(s,t) = v(s,t) + h(t) + c(s) \tag{2}$$

where $c(s)$ denotes the initial conditions for the growth, $h(t)$ denotes a uniform growth in all directions and $v(s,t)$ is the growth function. Because $v(s,t)$ is a periodic function in $\theta(s)$ due to

$$v(s,t) = v(s+S,t) \tag{3}$$

a Fourier expansion can be used to replace it, and Eq. (2) can then be rewritten as:

$$r(s,t) = \sum_k \Big(g_{k,1}(t) cosk\theta(s) + g_{k,2}(t) sink\theta(s)\Big) + h(t) + c(s) \tag{4}$$

where $g_{k,1}(t), g_{k,2}(t)$ are the Fourier coefficients that are functions of time t, which extends the traditional constant Fourier coefficients. Theoretically, Eq. (4) can simulate arbitrary star-shaped pattern, along with arbitrary evolution characteristics. This model can represent

non-star-shaped patterns when $\theta(s)$ is chosen to be nonlinear in S. Moreover, this model can easily be extended to the three-dimensional case, which will be investigated in a further study. Starting from a circle, the interface displacement of four simulation examples in the two-dimensional case with different growth roles are shown in Figure 1.(a)-(d), which demonstrate that this kind of model can simulate complex crystal forms with an arbitrary number of branches. Figure 1.(e) also shows an example in three-dimensions where the form and distribution of the branches are very similar to the real crystal cluster, shown in Figure 1.(f).

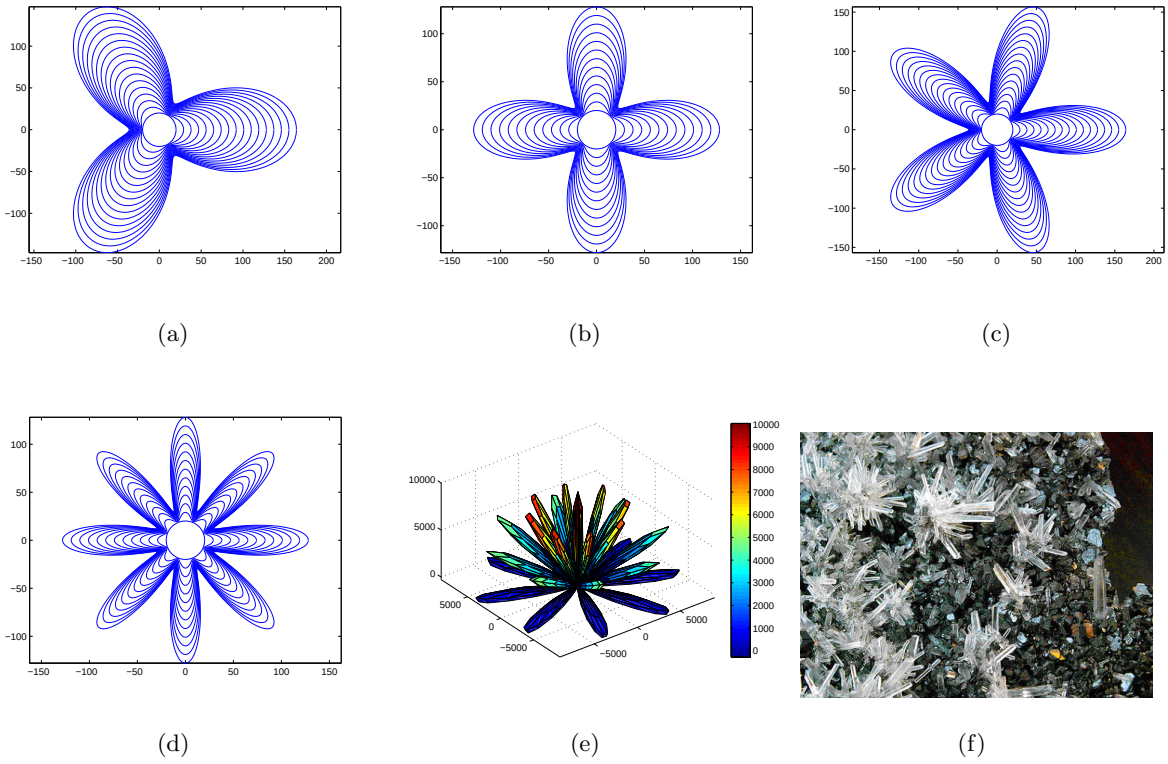

Figure 1: (a)-(d) Interface displacements of simulation examples by Eq. (4) in two-dimensions; (e) Snapshot of simulation example in three-dimensions; (f) Snapshot of a real crystal cluster.

3 Identification of the Radius-vector Function

The final purpose of this approach is to identify $r(s,t)$ directly from the observed data. Equation (4) is a static model where the coefficients and terms are time varying. Such a model often has less explanatory power in multi-step ahead predictions than a dynamic model. To solve this problem, this paper proposes a recursive model as an alternative and replace Eq. (4).

The derivative from Eq. (4) is given by:

$$\dot{r}(s,t) = \sum_k \left(\dot{g}_{k,1}(t) cosk\theta(s) + \dot{g}_{k,2}(t) sink\theta(s) \right) + \dot{h}(t) \tag{5}$$

A discrete recursive model therefore can be expressed as

$$r(s,t) = \sum_{i,k} a_{i,k} r(s,t-i) cosk\theta(s) + \sum_{i,k} b_{i,k} r(s,t-i) sink\theta(s) + h(t) + d(s) \tag{6}$$

where $a_{i,k}, b_{i,k}$ are the unknown Fourier coefficients. Eq. (6) can be identified directly from observed data using term selection and parameters estimation methods, and the many analytic methods which have been developed for dynamic models can then be applied to analyse and to help understand the observed system.

Given a group of observed data (r_j, θ_j, t_j), where j denotes the time index, the actual terms of Eq.(6) can be selected using the Orthogonal Least Squares routine (OLS) by ranking the candidate terms based on the Error Reduction Ratio (ERR), and then estimating the unknown parameters.

The selection of candidate terms is always very important in identification of a spatio-temporal system [Zhao and Billings, 2006]. There are two parameters which determine the candidate terms: D, the maximal time lag and K, the maximal value of k. The selection of K can be determined by the number of the branches and D is always chosen 1 in this paper. An example of the identification approach using simulation data will be employed to illustrate the approach. Starting from a circle, sixteen frames were generated using the rule

$$r(s,t) = 8tcos^2 2\theta(s) + 24tsin^2 3\theta(s) + t + 20$$

The generated patterns were sampled at θ by interval of 0.1 ($S = 20\pi$), and the displacement of the sampled interface is shown in Figure 2.(a).

Because there are six branches in the pattern, the initial candidate term set was therefore chosen as

$$\begin{aligned}
&\{1, \\
&cos\theta(s), cos2\theta(s), ..., cos6\theta(s), sin\theta(s), sin2\theta(s), ..., sin6\theta(s), \\
&r(s,t-1), \\
&r(s,t-1)cos\theta(s), r(s,t-1)cos2\theta(s), ..., r(s,t-1)cos6\theta(s), \\
&r(s,t-1)sin\theta(s), r(s,t-1)sin2\theta(s), ..., r(s,t-1)sin6\theta(s)\}
\end{aligned}$$

The selected terms and corresponding coefficients produced by OLS are shown in Table 1. The dynamic model can then be expressed using Eq.(7) as

$$r(s,t) = r(s,t-1) + 4cos4\theta(s) - 12cos6\theta(s) + 17 \tag{7}$$

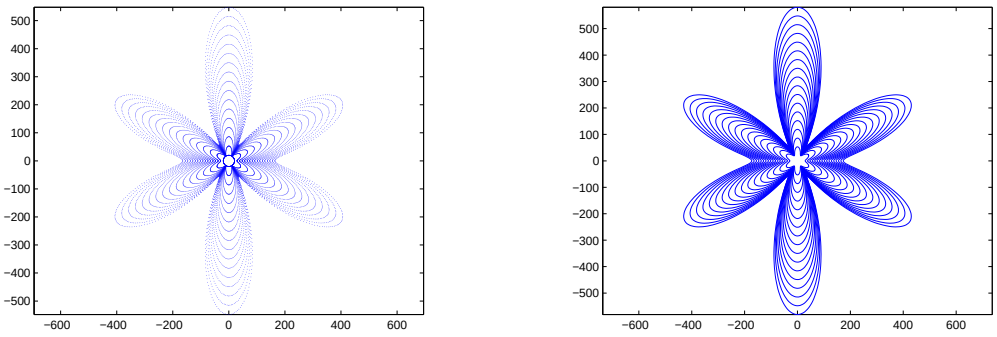

(a) (b)

Figure 2: (a)Observed data from a simulation example ; (b)Displacement of multi-step ahead prediction using the identified model (Eq.(7)).

Table 1: Results for the identification of simulation data using OLS

Term	ERR	Coefficient
1	0.813291	17
$cos6\theta(s)$	0.16545	-12
$cos4\theta(s)$	0.0184098	4
$r(s,t-1)$	0.00284968	1

To evaluate the identified model, starting from the same initial conditions as the simulation, for a group of patterns the multi-step ahead predictions using Eq.(7) and the displacement of the predicted interface were computed and are shown in Figure 2.(b). Inspection of the initial data and the multi-step ahead predictions shows that the identified model can fully describe the observed system. This is also reflected by the fact that the sum of the ERR values of the selected terms is 1, as shown in Table 1.

The second example using this approach is more challenging. This involves modelling a group of observed data from a real crystal growth experiment using NH_4Cl [Dougherty and Lahir, 2005]. Figure 3.(a) shows the displacement of the interfaces which evolve from time step 1 to time step 16. Figure 3.(b) shows a snapshot of the crystal at time step 16. As a pre-processing step, the displacement was rotated and each branch was marked by the sequance $A, B, C, ...$, illustrated by Figure 4.(a). Inspection of Figure4.(a) shows that there are 18 branches including

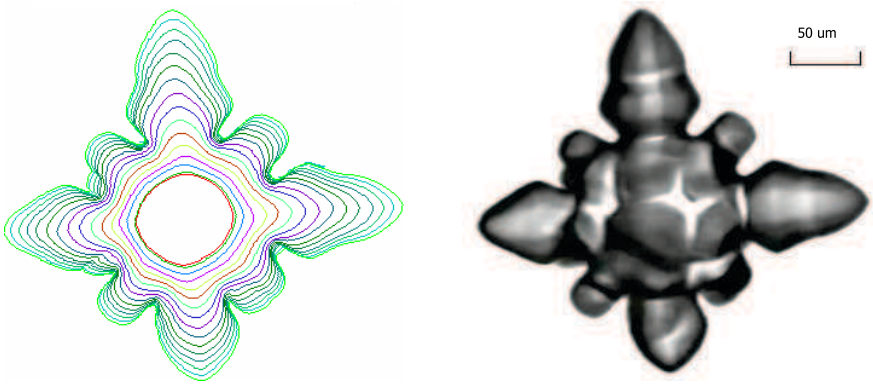

(a) (b)

Figure 3: (a) Displacement of the crystal interfaces for 16 time steps; (b) A snapshot of the crystal at time step 16.

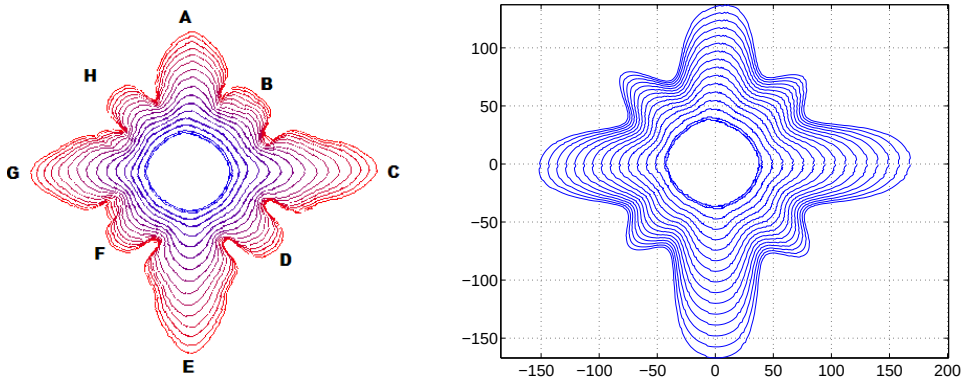

(a) (b)

Figure 4: (a) The displacement pattern for the real example after rotating;(b) The displacement pattern generated by the identified model.

the small bumps nearby tips, the initial candidate term set was therefore chosen as

$$
\begin{aligned}
&\{1,\\
&cos\theta(s), cos2\theta(s), ..., cos18\theta(s), sin\theta(s), sin2\theta(s), ..., sin18\theta(s),\\
&r(s,t-1),\\
&r(s,t-1)cos\theta(s), r(s,t-1)cos2\theta(s), ..., r(s,t-1)cos18\theta(s),\\
&r(s,t-1)sin\theta(s), r(s,t-1)sin2\theta(s), ..., r(s,t-1)sin18\theta(s)\}
\end{aligned}
$$

There is always a tradeoff between model efficiency and model complexity. For a real system, it is sometimes difficult to determine how many model terms should be chosen just in terms of the sum of ERR values. In this example, by choosing different numbers of terms, several models were identified and their performance based on multi-step ahead predictions were compared

using the Mean Square Error(MSE),

$$MSE(\hat{r}) = E(\hat{r} - r)^2$$

where $\hat{r}$ is the estimated value and r is the real value. Table 2 shows the MSE values of tip positions of eight branches in multi-step ahead predictions generated by models with a different number of terms. As expected, the MSE value decreases following the increment of the number

Table 2: Comparison of MSE values of multi-step ahead prediction generated by models with different numbers of terms

Number of terms	MSE
2	519.88
5	42.21
10	29.51
13	21.73
14	18.39
15	16.78
16	16.84
18	16.58

of terms. Notice that the model predictions show no significant improvement if the number of terms is larger than 15. For this example, the algorithm has therefore selected the most significant 15 terms from a total set of 56 possible model terms.

The final description of the identified model, the parameters of which were estimated using OLS after term selection, is presented in Table 3. To evaluate the identified model, starting from the same first and second frames as the observed data, fourteen multi-step ahead predictions were generated, and the displacement of the interfaces is shown in Figure 4.(b). A comparison between Figure 4.(a) and (b) shows that the identified model captures the main growth characteristics, such as the number of branches, asymmetrical growth speed among branches etc.. Moreover, the interface of the 14^{th} predicted frame is very close to the real data, which is always very difficult to achieve for multi-step ahead predictions. Figure 5 shows a comparisons of the radius-vector function between the reconstructed data and the real data at different times, where the dot curves indicate the contours from reconstructed data and the solid curves indicate the contours from real data. This also clearly indicates that the reconstructed contours are geometrically close to the contours of the real data.

As one of the most important variables to describe crystal growth, the evolution of the branch

Table 3: Results for the identification of the real data using OLS

Term	ERR	Coefficient
$r(s,t-1)$	0.9983	0.965883
1	0.000277527	7.55169
$r(s,t-1)cos4\theta(s)$	0.000289163	0.0283955
$cos8\theta(s)$	0.000126877	0.0834899
$r(s,t-1)sin\theta(s)$	$2.04141e-005$	-0.00607122
$cos\theta(s)$	$1.16115e-005$	0.395276
$r(s,t-1)cos12\theta(s)$	$1.03818e-005$	-0.0168275
$r(s,t-1)cos8\theta(s)$	$9.21077e-006$	0.019635
$r(s,t-1)sin3\theta(s)$	$8.7034e-006$	0.0044834
$r(s,t-1)cos5\theta(s)$	$4.20299e-006$	0.00309449
$r(s,t-1)sin6\theta(s)$	$4.13019e-006$	0.00299367
$cos12\theta(s)$	$3.55307e-006$	0.806516
$sin5\theta(s)$	$3.50071e-006$	-0.227734
$r(s,t-1)cos10\theta(s)$	$2.59922e-006$	0.00241942
$cos3\theta(s)$	$1.00339e-006$	0.120467

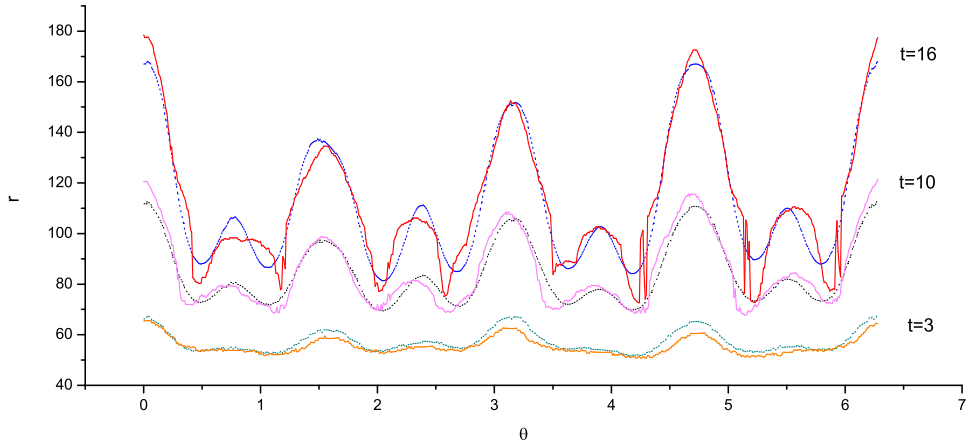

Figure 5: Radius vs vector of real data and reconstructed data at different times

tips of the predictions and the observed data were compared and the results are illustrated in

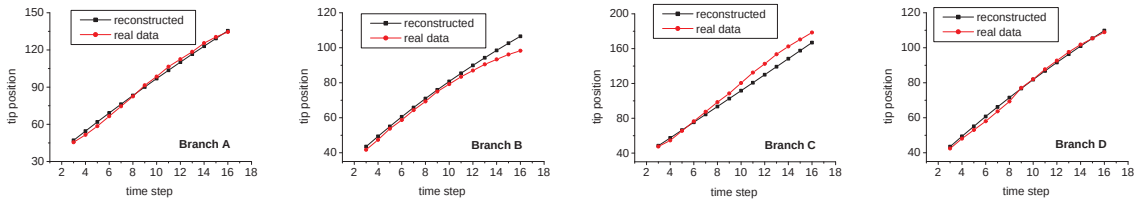

(a) $ARE = 0.02530$ (b) $ARE = 0.03760$ (c) $ARE = 0.05777$ (d) $ARE = 0.01932$

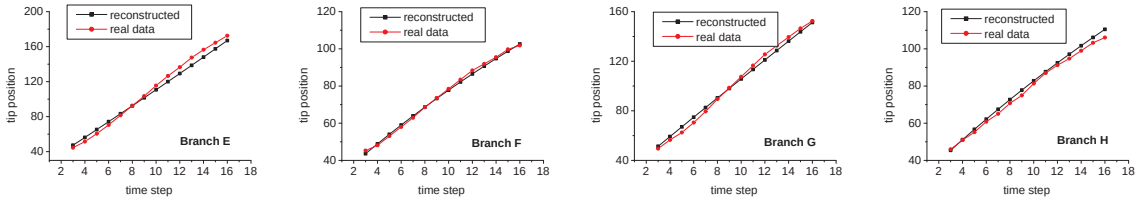

(e) $ARE = 0.04744$ (f) $ARE = 0.01374$ (g) $ARE = 0.03084$ (h) $ARE = 0.02372$

Figure 6: Comparison of real position and predicted position of each tip over time

Figure 6 along with the corresponding averaged relative error(ARE). ARE can be expressed as

$$ARE(\hat{r}) = E(\frac{|\hat{r} - r|}{r})$$

All values of ARE for the eight branch tips are below 0.06, which indicates that the model describes the tip growth well.

4 Conclusions

Initially, the contour of the crystal was parameterised in polar coordinates as a general model, which can reconstruct an arbitrary closed contour. A radius-vector based function was then proposed to describe a special case: star-shaped patterns. Evolution of the contour was expressed in a polynomial form, where the growth was decomposed into three parts: initial conditions, uniform growth and directional growth. As $r(s)$ at time t is always a periodic function, the Fourier expansion was employed to fit the contour of the object. To describe the evolution of the interface, the Fourier coefficients became functions of time rather than constants. To understand the dynamics characteristics of the observed data, this paper also introduced a recursive model which can fully substitute the static model. This was illustrated using a simulation example. The candidate model terms was determined by the number of branches in the patterns. Orthogonal Least Squares was then used to select significant terms from a pool of candidate terms based on the Error Reduction Ratio. Identification of the observed data from

a real crystal experiment shows the accuracy of the identified model depends on the complexity of the model. To achieve an effective model with the least number of terms, the MSE was employed to evaluate the performance of the models. Results of the multi-step ahead prediction clearly show the identified model can capture most growth characteristics in both spatio and temporal planes.

Both studied examples in this paper are based on star-shaped patterns, which is normal in the early stages of crystal growth. In this case, $\theta(s)$ is linear in s and independent of time t. This model can also describe non-star-shaped patterns when $\theta(s)$ is nonlinear in s or dependent on t. In this case, the identification includes not only the determination of $r(s,t)$, but also the determination of $\theta(s,t)$. This will be studied in future to consider more characteristics to describe the later stage - dendritic formation. Identification of real systems is often very difficult because of the many factors involved, such as rotation of the crystal, aberrations in the lens or other equipment factors. Predicting anything many steps ahead is always going to show up increasing errors as the prediction horizon increases. This is an inevitable consequence of slight model errors, noise effects etc. Many more experiments need to be conducted and the link between the identified model and the environmental and control parameters needs to be investigated in further studies.

Acknowledgment

The authors gratefully acknowledge that part of this work was financed by Engineering and Physical Sciences Research Council(EPSRC), UK, and by the European Research Council(ERC).

References

Dougherty A and Nunnally T. The transient growth of ammonium chloride dendrites. *Journal of Crystal Growth*, 300(2):467–472, 2007.

V Bisker-Leib and M. F. Doherty. Modeling the crystal shape of polar organic materials:prediction of urea crystals grown from polar and nonpolar solvents. *Crystal Growth & Design*, 1(6):455–461, 2001.

V Bisker-Leib and M. F. Doherty. Modeling crystal shape of polar organic materials: Applications to amino acids. *Crystal Growth & Design*, 3(2):222–237, 2003.

D.Mollison. Conjecture on the spread of infection in two dimensions disproved. *Nature*, 240: 467–768, 1972.

Andrew Dougherty and Mayank Lahir. Shape of ammonium chloride dendrite tips at small supersaturation. *Journal of Crystal Growth*, 274(1-2):233–240, 2005.

Murray Eden. A two-dimensional growth process. *4th. Berkeley symposium on mathematics statistics and probability*, 4:223–239, 1956a.

Murray Eden. A probabilistics model for morphogenisis. *Symposium on imformation theory in bilogy*, 29-31:359–370, 1956b.

WL George and JA Warren. A parallel 3d dendritic growth simulator using the phase-field method. *Journal Of Computational Physics*, 177(2):264–283, 2002.

H Hou, DY Ju, and YH Zhao. Numerical simulation for dendrite growth of binary alloy with phase-field method. *Journal Of Materials Science & Technology*, 20(1):45–48, 2005.

Buchmann M and Rettenmayr M. Rapid solidification theory revisited - a consistent model based on a sharp interface. *Scripta Materialia*, 57(2):169–172, 2007.

M Maalmi, A Varma, and WC Strieder. The sharp interface model - zero-order reaction with volume change. *Industrial & Engineering Chemistry Research*, 34(4):1114–1125, 1995.

M.J.Vold. Computer simulation of floc formation in a colloidal suspension. *Journal of colloid science*, 18:684–695, 1963.

M.Korenberg and S.A.Billings. Orthogonal parameter estimation algorithm for nonlinear stochastic systems. *International journal of control*, 48(1):193–210, 1988.

P.Meakin. Cluster-growth processes on a two-diemensional lattice. *Physical Review*, B28: 6718–6732, 1983.

R.Kobayashi. Modelling and numerical simualtions of dendritic crystal growth. *Phsical D*, 63: 410–423, 1993.

S.A.Wolfram. *A new kind of science*. Champaign: Wolfram Media, 2002.

T Takaki, T Fukuoka, and Y Tomita. Phase-field simulation during directional solidification of a binary alloy using adaptive finite element method. *Journal Of Crystal Growth*, 283(1-2): 263–278, 2005.

T.Williams and R.Rjerknes. Stochastic model for abnormal clone spread through epithelial based layer. *Nature*, 236:19–21, 1972.

T.A. Witten and L.M. Sander. Diffusion-limited aggregation, a kinetic critical phenomenon. *Physical Review Letters*, 47:1400–1403, 1981.

Y. Zhao and S.A. Billings. Neighborhood detection using mutual information for the identification of cellular automata. *IEEE Transactions on Systems, MAN, and CyberneticsPart B*, 36(2):473–479, 2006.

Y. Zhao, S.A. Billings, D. Coca, R.I.Ristic, and L.DeMatos. Identification of the transition rule in a modified cellular automata model: The case of dendritic nh4br crystal growth. *International Journal of Bifurcation and Chaos*, 19(7):2295–2305, 2009.